Distributed Matching Network Design for Broadband Power Amplifiers

Yuan Zhuang, Zhouxiang Fei, Anqi Chen, Yi Huang and Jiafeng Zhou
University of Liverpool, Department of Electrical Engineering and Electronics, Liverpool, UK
Jiafeng.zhou@liverpool.ac.uk

***Abstract*— This paper presents a distributed matching network design method for the realization of broadband high-efficiency power amplifiers (PAs). Source-pull and load-pull simulations are employed to determine the optimal input and output impedances of a GaN transistor across 0.3-2.3 GHz. With the optimal source and load impedances across the desired bandwidth, the proposed method can be used to compute and optimize the distributed matching network directly without requiring close-form initial element values. This method will enable a PA to achieve high power added efficiency (PAE) over an ultra-wide bandwidth. A low-pass matching network is applied to implement the optimal impedances over the band. The measured results of the PA indicate a power gain of better than 10 dB and a typical output power of 20 W. The PAE is 59%-69% across a 153% bandwidth. The measurement demonstrates the excellence of the proposed method.**

***Index Terms*—Broadband; distributed matching network; high-efficiency; power amplifier.**

I. Introduction

Power amplifiers (PAs) are essential devices for communication systems. The features of a PA in terms of operational bandwidth, power gain, linearity, output power level and power added efficiency (PAE) could significantly affect the overall performance of a system. Particularly, a high-power, high-efficiency broadband PA is in high demanded by the industry and market. Designs reported in [1]-[3] use filter-type matching networks (MN) to match the fixed optimal impedance at the center frequency for the PA over a wide bandwidth. With this technique, optimal performance can be achieved at the center frequency by compromising the performance at other frequencies over the band at a reasonable level. However, these approaches are not suitable for designs where the optimal impedances at different frequencies are not close to each other, which is almost always the case in multi-octave PA designs.

Conventionally, this kind of multi-objective matching problem can be solved by computer-aided design (CAD) tools to realize a global solution. However, CAD tools require the selection of initial element values to start the optimization. Without reasonable initial values, CAD tools will not be able to find proper design values. This paper introduces a simple and efficient approach to compute the distributed matching network for wideband high efficiency PAs without needing the initial guess of element values. The detailed design method is presented and explained in this paper, including how to match the impedance with a distributed low-pass LC-ladder MN. A PA operating over 0.3-2.3 GHz with 58%-69% PAE at a typical output power of 43 dBm has been designed and measured to validate the method.

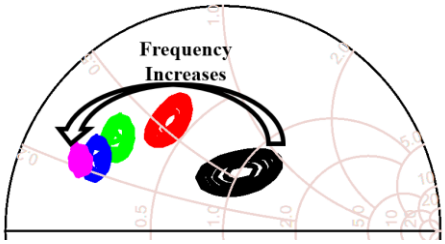

Fig. 1. PAE impedance contours of a CGH40025 vary with frequency.

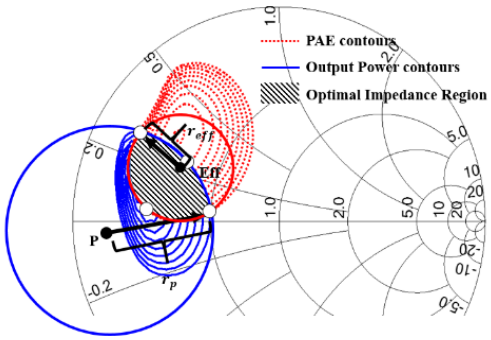

Fig. 2. PAE and output power contours of a CGH40025 at 1 GHz and the optimal impedance region.

II. Proposed Method and PA Design

A. Load-Pull Simulation and Optimal Impedances

Across a wide bandwidth, the optimal impedances of a transistor at different frequencies are not close to each other as depicted in Fig. 1. Moreover, the optimal impedances for high efficiency and high output power are not identical. The high PAE contours of a CGH40025 from Cree at 1 GHz are shown in Fig. 2. The contours are quite different from each other across the band. To achieve high efficiency across a wide band, the optimal impedance should not be a fixed value at each frequency section. Hence, several frequency-dependent optimal impedances across the operational band should be defined, which allow the PA to have performance better than the lowest acceptable performance.

The entire operational bandwidth should be divided into multiple frequency sections depending on the required bandwidth and the variation of the optimal impedances. For each frequency section, the shared area of the high output power and high PAE contours can be selected as the optimal impedances for this frequency section.

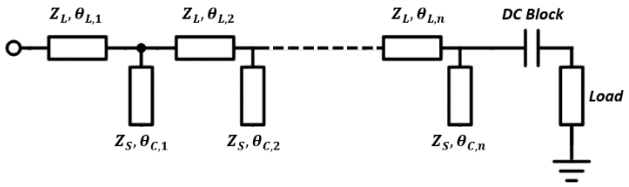

Fig. 3. A distributed low-pass MN with a lumped DC block capacitor.

B. Matching Network Design Method

Once the optimal impedance regions are defined, the next task is to realize the desired impedances using a proper matching circuit topology. A distributed series and shunt low-pass ladder network is selected to implement the MN which can satisfy the matching and filtering requirement simultaneously [4]. The MN has lumped capacitor to proivde electrical isolation between the radio frequency signal and direct current as shown in Fig. 3. The MN can be treated as a cascaded structure of several transmission lines interconnected with a lumped DC block capacitor. The ABCD matrix of the MN can be expressed as:

$$\begin{bmatrix} A(\omega_k) & B(\omega_k) \\ C(\omega_k) & D(\omega_k) \end{bmatrix}_{LC} = \left(\prod_{i=1}^{n} \begin{bmatrix} \cos(\frac{\omega_k}{2\pi}\theta_{L,i}) & jZ_L \sin(\frac{\omega_k}{2\pi}\theta_{L,i}) \\ j\frac{\sin(\frac{\omega_k}{2\pi}\theta_{L,i})}{Z_L} & \cos(\frac{\omega_k}{2\pi}\theta_{L,i}) \end{bmatrix} \cdot \begin{bmatrix} 1 & 0 \\ j\frac{\tan(\frac{\omega_k}{2\pi}\theta_{C,i})}{Z_C} & 1 \end{bmatrix} \right) \cdot \begin{bmatrix} 1 & \frac{1}{j\omega_k C_{DC}} \\ 0 & 1 \end{bmatrix} \quad (1)$$

where $\omega_k=2\pi f_k$, k is the number of the frequency sections and n is the number of ladder sections used in the network. Z_L and Z_C are the characteristic impedances of the series lines and the shunt stubs, respectively; θ_L and θ_C represent the electrical length of the series transmission lines and open stubs, respectively. Z_{load} is the termination impedance of the MN, 50 Ω in this paper. With the expression in (1), the input impedance at each frequency section of the MN can be calculated. If the corresponding Z_{in} of the MN at each frequency section is inside the corresponding optimal impedance region, the MN will provide optimal performance for the device.

Therefore, the problem then is to find the proper characteristic impedances and electrical lengths for series lines and shunt stubs of the MN. The series lines should have high impedance to behave inductively and the shunt stubs should have low impedance to act like capacitors. In this paper, the series line and shunt stub impedances are chosen to be Z_L=25 Ω and Z_C=80 Ω respectively. Then, to satisfy the predefined optimal impedance contours, the proper electrical lengths of the MN can be denoted as $\theta_L=\{\theta_{L,1}, \theta_{L,2}, \ldots \theta_{L,n}\}$ and $\theta_C=\{\theta_{C,1}, \theta_{C,2}, \ldots \theta_{C,n}\}$, where n is the number of the ladder sections used in the MN. The elements in variable θ_L and θ_C are denoted by subsets as $\theta_{L,m}=\{\theta_{L,n}^{(1)}, \theta_{L,n}^{(2)}, \ldots \theta_{L,n}^{(m)}\}$ and $\theta_{C,m}=\{\theta_{C,n}^{(1)}, \theta_{C,n}^{(2)}, \ldots \theta_{C,n}^{(m)}\}$, where m is the number of samples in the subset. Due to the possible electrical length varies from 0 degree to 180°, we divide all the possible values of electrical lengths into m samples as shown in the **Error! Reference source not found.**. The dimensions of the variable can be equivalently visualized using the two-dimensional θ_L – θ_C plane, where θ_L and θ_C represent the electrical length for series transmission lines and open stubs respectively. This plane can be divided into parts based on the distance to points

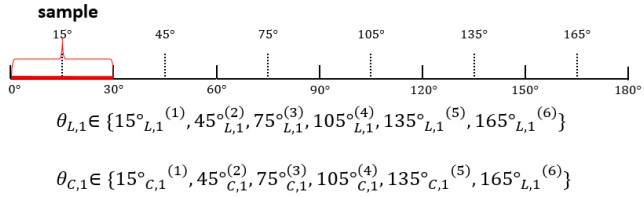

Fig. 4. Example of sampled subset of the electrical length.

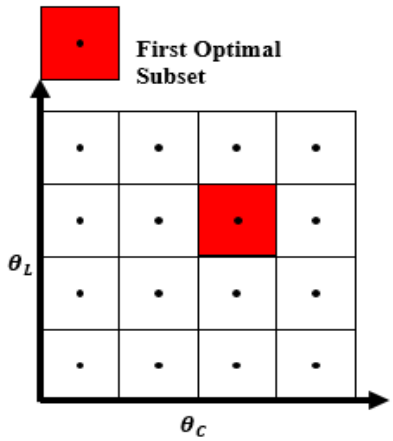

Fig. 5. Illustration of the optimization of electrical lengths and the optimal subset.

Table I: Optimal Subsets for the OMN

	$\theta_{L,1}$	$\theta_{L,2}$	$\theta_{L,3}$	$\theta_{L,4}$	$\theta_{C,1}$	$\theta_{C,2}$	$\theta_{C,3}$	$\theta_{C,4}$
Subset1	15°	15°	15°	15°	45°	45°	15°	15°
Subset2	7.5°	2.5°	2.5°	10°	37.5°	32.5°	22.5°	17.5°
Subset3	**5°**	**2°**	**2.5°**	**6°**	**38°**	**31°**	**23°**	**19°**

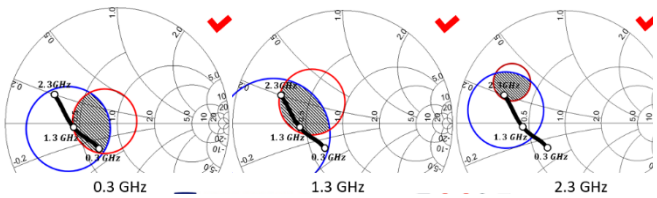

Fig. 6. The input impedance of the OMN across the bandwidth.

in a specific subset of the plane with the method reported in [5] as shown in Fig. 5. With the sampled electrical length values, use (1) to calculate the corresponding input impedance $Z_{in}(\omega_k)$ of each subset. The shortest Ecudiclne distance from the input impedance to the output power and PAE contour can be calculated.

If the input impedance of the mth subset is in the optimal impedance regions over the desired band. This subset will be used to synthesize the MN. If no subset can meet the requirements, the shortest Ecudiclne distance from the input impedance to the optimal impedance region should be calculated. The matching quality of the subset can be evaluated by:

$$\Lambda^{(m)} = \sum_{i=1}^{k} \left| d_{in}^{(m)}(\omega_i) \right|^2 \quad (2)$$

where the $d_{in}^{(m)}(\omega_i)$ is the shortest Euclidean distance from the input impedance of the mth subset at i^{th} frequency section to the corresponding optimal impedance region. The mth subset that has the minimum $\Lambda^{(m)}$ will be selected as the optimal

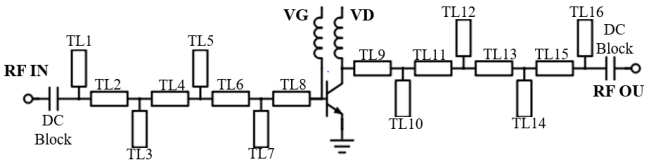

Fig. 7. A schematic of the PA.

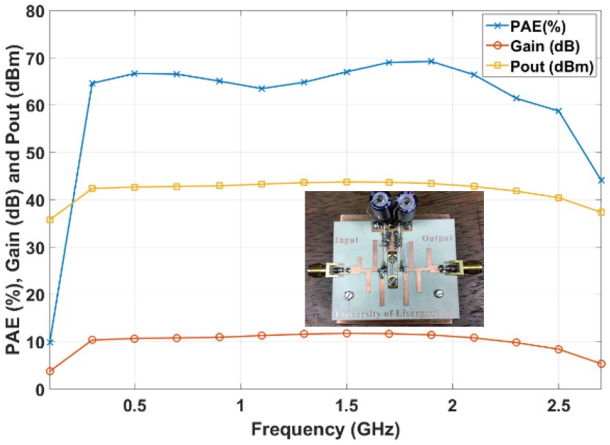

Fig. 8. Measured Gain, output power, PAE versus frequency and a photo of the fabricated PA.

subset for further optimization. Repeat the sampling of the optimal subset and selecting a new optimal subset until the requirements are satisfied. The computing process and input impedance of the designed MN across the desired band are illustrated in Fig. 6.

C. PA Design

A CGH40025F is chosen to realize the design. The PA was implemented on a 1.52 mm thick Rogers 4350B substrate with ε_r=3.48 and 1 oz/sqft copper. The PA was designed to operate from 0.3 GHz to 2.3 GHz with an output power greater than 40 dBm and a PAE better than 60%. A 4th-order low-pass structure as shown in Fig. 3. was applied to realize the output matching network (OMN). The number of samples m for each θ_L and θ_C are chosen to be 6 as illustrated in Fig. 4. Following the procedure described above, three optimal subsets of the electrical length of the transmission lines and open stubs are obtained as listed in Table I. For the third optimal subset, the corresponding input impedance of the OMN are all inside the predefined optimal impedance region as shown in Fig. 6. Hence, the value in the third optimal subset is suitable to realize the OMN. The input matching network was designed likewise.

D. Measurement Results

A schematic of the PA is shown in Fig. 7. A photo of the fabricated PA is shown in Fig. 8. The gate of the transistor was biased at -3 V, and the drain voltage was 28 V. The measured PAE, gain and output power across the operational band are shown in Fig. 8. The broadband PA has a PAE higher than 59% over the desired bandwidth. The PAE is slightly lower at the high-frequency end. The gain is better than 10 dB, and the corresponding output power varies from 40 dBm to 43.5 dBm. The performance of this PA is compared with other reported broadband high-efficiency PAs as listed in Table II. The proposed PA can achieve desired performance over the widest bandwidth. The broadband high-efficiency performance of this PA has validated the proposed design method.

Table II: Broadband High-Efficiency PAs

Ref.	Freq (GHz)	Fractional BW	Gain (dB)	P_{out} (W)	Eff. (%)
[2]	1.9-4.3	77%	9-11	10-15	57-72*
[1]	0.36-0.79	75%	5-14	10	30-81^
[6]	0.9-2.2	84%	10-13	10-20	63-89*
[7]	1.3-3.3	87%	10-13	10-11	59-79^
[8]	0.9-3.2	112%	10-14	9.1-20.4	52-85^
[9]	0.8-4	133%	5-7	1-2	40-55*
This work	**0.3-2.3**	**153%**	**10-12**	**16-22**	**59-69^**

*: Drain Efficiency，^: Power Added Efficiency

III. Conclusion

This paper has presented a simple and effective method of designing wideband high-efficiency PAs. The optimal source and load impedances for a transistor have been defined by optimal impedance regions instead of fixed values based on source-pull/load-pull simulations. A distributed low-pass ladder network has been applied to match the predefined optimal impedance regions. A method of synthesizing the MN has been presented which can computed the MN values directly without initial guess. The designed PA has been fabricated and measured. The large signal experimental results have shown a PAE of 59-69%, a gain better than 10 dB and a typical output power of 20 W over a wide bandwidth from 0.3 GHz to 2.3 GHz. The state-of-the-art performance is better than any other reported works. The results have indicated the potential of the proposed method for future communication system applications where high-efficiency and wideband amplifiers are needed.

References

[1] J. Zhou, K. A. Morris, G. T. Watkins and K. Yamaguchi, “Improved reactance-compensation technique for the design of wideband suboptimum class-E power amplifiers,” *IEEE Trans. Microw. Theory Techn.*, vol. 63, no. 9, pp. 2793–2801, Sep. 2015.

[2] P. Saad, C. Fager, H. Cao, H. Zirath, and K. Andersson, “Design of a highly efficient 2–4-GHz octave bandwidth GaN-HEMT power amplifier,” *IEEE Trans. Microw. Theory Tech.*, vol. 58, no. 7, pp. 1677–1685, Jul. 2010.

[3] Y. Zhuang, J. Zhou, Y. Huang and A. Chen, “Design of a broadband high-efficiency GaN power amplifier for GNSS applications,” *IEEE MTT-S International Wireless Symposium,* 2016.

[4] G. L. Matthaei, “Tables of Chebyshev impedance-transformation networks of low-pass filter form,” *Proc. IEEE*, vol. 52, no. 8, pp. 939–963, 1964.

[5] S. Sarkar, J. E. Warner, W. Aquino, and M. Grigoriu, “Stochastic reduced order models for uncertainty quantification of intergranular corrosion rates,” *Corrosion Science*, vol. 80, pp. 257-268, Mar. 2014.

[6] K. Chen and D. Peroulis, “Design of highly efficient broadband class-E power amplifier using synthesized low-pass matching networks,” *IEEE Trans. Microw. Theory Techn.*, vol. 59, no. 12, pp. 3162–3173, Dec. 2011.

[7] K. Chen and D. Peroulis, “Design of broadband highly efficient harmonic-tuned power amplifier using in-band continuous class-F-1/*f* mode transferring,” *IEEE Trans. Microw. Theory Techn.*, vol. 60, no. 12, pp. 4107–4116, Dec. 2012.

[8] Z. Dai, S. He, F. You, J. Peng, P. Chen and L. Dong, “A New Distributed Parameter Broadband Matching Method for Power Amplifier via Real Frequency Technique,” *IEEE Trans. Microw. Theory Tech.*, vol. 63, no. 2, pp. 449–458, Feb. 2015.

[9] P. Colantonio, F. Giannini, R. Giofre, and L. Piazzon, “High-efficiency ultra-wideband power amplifier in GaN technology,” *Electron. Letter.,* vol. 44, no. 2, pp. 130–131, Jan. 2008.